ORIGINAL PAPER

Size-dependent photosynthetic performance in the giant clam *Tridacna maxima*, a mixotrophic marine bivalve

Annie Ji-Yih Yau · Tung-Yung Fan

Abstract Giant clams form a symbiosis with photosynthetic algae of the genus *Symbiodinium* that reside in clam mantle tissue. The allometry of symbiont photosynthetic performance was investigated as a mechanism for the increasing percentage of giant clam carbon respiratory requirements provided by symbionts as clam size increases. Chlorophyll fluorescence measurements of symbionts of the giant clam *Tridacna maxima* were measured during experiments conducted in September of 2009 using specimens 0.5–200 g tissue wet weight (3–25 cm long), collected from waters around southern Taiwan (N 21°36′, E 120°47′) from July to August of 2009. Light-dependent decreases in effective quantum yield ($\Delta F/F_m'$) calculated as the noontime maximum excitation pressure over PSII (Q_m), relative electron transport rates (rETR), and dark-adapted maximum quantum yield (F_v/F_m) all varied as a quadratic function of clam size. Both Q_m and rETR increased as clam size increased up to $\sim$10–50 g then decreased as clam size increased. F_v/F_m decreased as clam size increased up to $\sim$5–50 g then increased as clam size increased. Chlorophyll fluorescence measurements of rETR were positively correlated with gross primary production measured during chamber incubations. Overall, symbionts of mid-sized clams $\sim$5–50 g exhibited the highest light-dependent decreases in effective photosynthetic efficiencies, the highest relative electron transport rates, and the lowest maximum photosynthetic efficiencies, and symbiont photosynthetic performance is allometric with respect to host clam size.

Introduction

Endosymbiotic relationships between invertebrates and unicellular algae are common on coral reefs and can be found in reef-building corals, soft corals, sponges, anemones, and giant clams (Trench 1993; Venn et al. 2008). All ten species of giant clams (family Tridacnidae, genera *Tridacna* and *Hippopus*) contain symbiotic photosynthetic algae of the genus *Symbiodinium* (Jeffrey and Haxo 1968), which reside intercellularly within a special tubular system in the exposed mantle tissue connected to the stomach (Norton et al. 1992). *Symbiodinium* (hereafter referred to as symbionts) are obtained by juvenile giant clams via horizontal transfer from the water column through filter feeding (Fitt and Trench 1981). Giant clams obtain nutrients through both phototrophic and heterotrophic pathways: they acquire glucose from their symbionts (Ishikura et al. 1999) and continuously filter feed phytoplankton and other similarly sized particles from surrounding water (Klumpp et al. 1992; Hawkins and Klumpp 1995). This combination of phototrophic and heterotrophic pathways is thought to be the reason why giant clams have fast growth rates compared with other bivalves (e.g. Klumpp and Griffiths 1994) and thrive in the oligotrophic waters of coral reefs, even forming reefs composed mainly of giant clams (Andrefouet et al. 2005).

Despite retaining complete functional filter feeding and digestive systems typical of other heterotrophic bivalves

Communicated by M. Kühl.

A. J.-Y. Yau (✉)
Bren School of Environmental Science and Management,
University of California, Santa Barbara, CA 93106-5131, USA
e-mail: ayau@bren.ucsb.edu

T.-Y. Fan
National Museum of Marine Biology and Aquarium,
2 Houwan Road, Checheng, Pingtung 944,
Taiwan, People's Republic of China

(Morton 1978; Reid et al. 1984), giant clams rely heavily on their symbionts that can provide over 100% of a giant clam's carbon respiratory requirements and provide an increasing percentage of these requirements as the clam grows in size, with the exact proportions varying from one clam species to another (Fisher et al. 1985; Klumpp et al. 1992; Klumpp and Griffiths 1994; Klumpp and Lucas 1994). Similarly, the percentage of clam nitrogen requirements for growth and metabolism provided by symbionts increases as clam size increases (Hawkins and Klumpp 1995). Defining allometry as the non-linear scaling of a morphological or physiological characteristic with body size, and isometry as the linear scaling of a characteristic with body size, the symbiont contribution to giant clam respiratory and metabolic requirements increases allometrically as clam size increases.

Mechanisms causing this size-dependent shift in symbiont contribution are unknown but are possibly attributed to the allometry of giant clam physiology and symbiont photophysiology. Giant clams have fewer symbionts per unit clam biomass as they increase in size (Fisher et al. 1985; Fitt et al. 1993; Griffiths and Klumpp 1996), while the concentration of the photosynthetic pigment chlorophyll *a* within these symbionts does not change as a function of clam size (Griffiths and Klumpp 1996). As such, fewer symbionts are contributing increasingly higher proportions of clam respiratory requirements, and it is possible that changes in symbiont photosynthetic performance are responsible for this allometric relationship. A previous study used chamber incubations to determine photosynthesis (gross oxygen evolution per symbiont) decreased allometrically as clam size increased in *Tridacna gigas* (Fisher et al. 1985), but only tested a portion of the full size range of *T. gigas* (1–38 cm, when their maximum size is 137 cm (Rosewater 1965)), and only measured photosynthesis under one relatively high irradiance level (1,000 μmol photons m^{-2} s^{-1}). To complement the results of Fisher et al. (1985), we examined the photosynthetic performance of giant clam symbionts across the entire size range of the small giant clam *T. maxima* under various light conditions. We used a different approach, chlorophyll fluorescence analysis, to measure photosynthetic performance as the efficiency of photosystem II photochemistry and relative electron transport rates.

Chlorophyll fluorescence is the re-emission by chlorophyll of absorbed light as light of a longer wavelength and increases when there is a decrease in the amount of absorbed light energy that is used for photosynthesis or dissipated as heat (for reviews on the theoretical background, techniques, and applications of chlorophyll fluorescence see Maxwell and Johnson (2000) and Schreiber (2004)). Chlorophyll fluorescence yields measurements of photosynthetic performance and efficiency (defined here as the efficiency of PSII photochemistry), and several studies have found significant correlations of chlorophyll fluorescence with rates of net primary production for algae (Beer et al. 2000) and corals (Hoogenboom et al. 2006), and with rates of gross primary production for giant clams (Jantzen et al. 2008).

Chlorophyll fluorescence, or simply fluorescence, can easily be measured using pulse amplitude modulated fluorometers (PAM) that function by emitting light of a certain wavelength and measuring the amount of light re-emitted at longer wavelengths. Several studies have used portable fluorometers to investigate the photosynthetic performance of giant clams (Elfwing et al. 2002; Elfwing et al. 2003; Jantzen et al. 2008; Richter et al. 2008) and have confirmed that fluorescence measurements can reveal differences in photosynthetic performance under different environmental conditions and between species (e.g. Elfwing et al. 2003; Jantzen et al. 2008). Each of these studies focused on one size of giant clam, ranging from 14 to 16 cm long for *T. gigas* (Elfwing et al. 2002, 2003) to 11 to 12 cm long for *T. maxima* and *T. squamosa* (Jantzen et al. 2008). As such, size dependency in chlorophyll fluorescence has not been tested for giant clams. We used chlorophyll fluorescence measurements of the efficiency of photosystem II photochemistry and relative electron transport rates to determine the photosynthetic performance of giant clam symbionts across the size range of the small giant clam *T. maxima* under various light conditions.

Materials and methods

Investigated specimens

Specimens of the small giant clam, *Tridacna maxima*, were collected at water depths of 3–10 m from fringing coral reefs around southern Taiwan (N 21°36′, E 120°47′) from July to August of 2009. This species of giant clam is commonly found on reefs worldwide as it has the widest geographic distribution within its family (Rosewater 1965). Collected clams ranged from 3 to 25 cm in shell standard length (the maximum anterior-posterior distance excluding scutes), equivalent to 0.5–200 g tissue wet weight ($n = 25$ total). The average maximum length of this species is ~25–30 cm (Rosewater 1965), so specimens we collected spanned the entire size range from juveniles to mature adults. Experiments ran in September of 2009 at the National Museum of Marine Biology and Aquarium, Taiwan, ROC. Clam shells were cleaned with a brush to remove all epibionts prior to measuring total standard length and were cleaned again immediately prior to any experimental measurements. To avoid killing all specimens, a few additional clams of various sizes were

collected and dissected to determine the following power relationship between standard length in cm (L) and tissue wet weight in g (W): $W = 0.0128\ L^{3.0374}$ ($n = 9$, $r^2 = 0.98$). Using this relationship, lengths were converted to tissue wet weight which we used to represent giant clam size in our analyses.

Immediately after collection, clams were placed in 280-L ($182 \times 59 \times 38$ cm, length $\times$ width $\times$ height), flow-through outdoor tanks in which the entire volume was replaced every 30 min. Clear plastic roofing reduced natural light levels by $\sim 40\%$ to minimize water temperature fluctuations. The mean maximum photosynthetically active radiation (PAR) experienced by the clams, as measured at noon over the course of a week with an LI-192 underwater quantum sensor (LI-COR, USA), was 654 ± 148 µmol photons m^{-2} s^{-1} ($\pm$SE) ($n = 7$). Tank temperatures, monitored with HOBO pendant loggers (Onset, USA) every 5 min, varied from 29.9 ± 0.3°C during the day to 29.6 ± 0.2°C at night ($\pm$ SE, $n = 620$). No additional food was provided beyond the natural amount in the unfiltered seawater flowing into the tanks. Clams were kept in these conditions ranging from 2 to 6 weeks, depending on their collection date, prior to any measurements to allow full acclimatization of symbionts to this light environment (Anthony and Hoegh-Guldberg 2003).

Fluorescence measurements

We used a submersible pulse amplitude modulated fluorometer (Diving-PAM; Walz, Germany) to measure the photosynthetic performance of symbionts of *T. maxima*. A simplified version of the Universal Sample Holder for the Diving-PAM (DIVING-USH; Walz, Germany) was used to access mantle tissue at a standardized distance of 1 cm without touching the sensitive tissue. Once the probe of the Diving-PAM was in place, we verified that clams maintained their mantle tissue expanded past the shell edge for at least 30 s before any measurements were taken. Only mantle tissue that was expanded and parallel to the surface of the water was sampled. Two types of measurements were taken with the Diving-PAM: PSII quantum yield (effective quantum yield, $\Delta F/F_m'$, and maximum quantum yield, F_v/F_m) and relative electron transport rates (rETR) as part of rapid light curves (RLCs). To obtain optimal fluorescence signals, the Diving-PAM was set to emit a saturating pulse of white light >5,000 µmol photons m^{-2} s^{-1} for 0.8 s, with settings for measuring light intensity and gain set to 12 and 7, respectively.

Quantum yield

Effective PSII quantum yield is a dimensionless ratio given by the equation: $\Delta F/F_m' = (F_m' - F)/F_m'$; where F_m' is the maximum fluorescence yield in the current light state, and F is the steady state fluorescence yield in this light adaptation state, monitored briefly before the saturation pulse (Genty et al. 1989). Maximum PSII quantum yield, F_v/F_m, is the quantum yield from a dark-adapted sample. These ratios of effective and maximum quantum yield measure the efficiency of photosystem II photochemistry as the proportion of light absorbed by photosystem II that is used for photosynthesis (Maxwell and Johnson 2000; Enríquez and Borowitzka 2010).

We measured effective PSII quantum yield ($\Delta F/F_m'$) of clams in the tanks on a cloudless day at 2.5-h intervals over a 12-h period, from 0700 to 1900 h on 1 September 2009. During each sampling period, between 3 and 5 measurements for each clam (1 to 2 measurements for the smallest clams <5 g tissue wet weight) were recorded from different areas of expanded mantle tissue and averaged for each clam at each sampling period following methods by Jantzen et al. (2008). PAR (in µmol photons m^{-2} s^{-1}) was simultaneously recorded during each $\Delta F/F_m'$ measurement using the Diving-PAM light sensor calibrated to an LI-192 underwater quantum sensor (LI-COR, USA). To test whether log-transformed tissue wet weight and/or PAR were significant predictors of $\Delta F/F_m'$, we performed a multiple regression of these two variables against $\Delta F/F_m'$, added second- and third-order terms for wet weight to the multiple regression, and used AICc to choose the most parsimonious model using R version 2.12.1 (R Development Core Team). AICc, or second-order Akaike information criterion, is a model selection metric where a model with the lowest AICc score is considered the best approximation for the data (Burnham and Anderson 2002).

We calculated the noontime reduction of $\Delta F/F_m'$, or maximum excitation pressure over photosystem II (Q_m), as $Q_m = 1 - (\text{noontime } \Delta F/F_m')/(F_v/F_m \text{ at dusk})$ (Iglesias-Prieto et al. 2004). Values of $\Delta F/F_m'$ at dusk (1900 h) are considered F_v/F_m because of low light levels (PAR < 45 µmol photons m^{-2} s^{-1}). As calculated here, Q_m serves as a proxy for non-photochemical quenching (NPQ), or the dissipation of light energy as heat, and Q_m values close to zero suggest photosynthetic rates are light limited while values close to 1.0 suggest photoinhibition (Iglesias-Prieto et al. 2004). To test whether Q_m varied with clam size, we again used R version 2.12.1 (R Development Core Team) to regress Q_m against log-transformed wet weight, adding second- and third-order terms for wet weight to the regression and using AICc to choose the most parsimonious model (Burnham and Anderson 2002).

Rapid light curves

We converted effective PSII quantum yield to relative electron transport rates (rETR, in µmol e$^-$ m^{-2} s^{-1}) using the

following equation: $rETR = \Delta F/F_m' \times PAR \times 0.5 \times A$; where PAR is the photosynthetically active radiation (in µmol photons m^{-2} s^{-1}), 0.5 represents the assumed equal distribution of electrons between photosystem II and photosystem I, and A is the light absorptance or fraction of light absorbed by the sample (clam tissue). The light absorptance for giant clams has not been determined, so we assumed a light absorptance of 1 throughout our measurements. Resulting calculated rETRs are approximations of the rate of electrons pumped through PSII, and changes in rETR reflect relative changes in photosynthetic rates (Enríquez and Borowitzka 2010). We measured rETR by conducting rapid light curves.

We conducted a rapid light curve (RLC) for each giant clam on 4 September 2009. Rapid light curves are rETR versus PAR and illustrate a sample's capacity to acclimate to a series of short light steps. In a RLC, the rETR measured at each light step indicates the actual state of photosynthetic electron transport compared to traditional P–I curves that illustrate the optimal steady state of photosynthesis at each light condition (Ralph and Gademann 2005). RLCs are generated by emitting eight consecutive flashes of artificial ("actinic") light of increasing intensity every 10 s, plus an initial measurement of photosynthetic yield recorded at ambient light before the light flashes begin. The actinic light levels were 300, 463, 657, 881, 1,293, 1,729, 2,559, and 3,667 µmol photons m^{-2} s^{-1} as measured by the Diving-PAM light sensor calibrated to an LI-192 underwater quantum sensor (LI-COR, USA). Because RLCs for 25 clams could not be conducted within a short time frame, clams were taken a few at a time from outdoor holding tanks and dark adapted for 30 min in similar tanks in a dark room prior to performing RLCs, in order to reduce the confounding effect of recent light history. The resulting dark-adapted rETR measurements represent the maximum rETR for PSII photochemistry at each light level (White and Critchley 1999). The initial measurement of photosynthetic yield at ambient light is dark adapted maximum quantum yield (F_v/F_m). We tested whether F_v/F_m changed as a function of clam size by regressing F_v/F_m against log-transformed wet weight, adding second- and third-order terms for wet weight to the regression, and using AICc to choose the most parsimonious model (Burnham and Anderson 2002) using R version 2.12.1 (R Development Core Team).

A standard rectangular hyperbola with an asymptotic maximum rETR value was fitted to an RLC generated for each clam using MATLAB 7.6.0.324 with Statistics Toolbox 6.2 (MathWorks, USA): $rETR = rETR_{max}(1-e^{-(\alpha*PAR/rETR_{max})})$; where $rETR_{max}$ is the maximum rETR at saturating light, PAR is irradiance, and α is the initial slope of the RLC before the onset of saturation (Ralph and Gademann 2005). There are two main parameters of these curves: $rETR_{max}$ (in µmol e^- m^{-2} s^{-1}) provides an estimate of the maximum electron transport rate achievable for each clam, and α (initial slope; change in rETR for a given change in PAR) indicates the maximum photochemical conversion efficiency. Because only 8 out of 25 RLCs reached saturation, we could not accurately extrapolate to $rETR_{max}$. Instead we compared values of rETR at the ecologically relevant irradiance level of 1293 µmol photons m^{-2} s^{-1}, which is the maximum irradiance level experienced by giant clams in their natural habitat (Buck et al. 2002; Jantzen et al. 2008). Similar methods were employed by Fisher et al. (1985) who measured P–I curves for T. gigas that did not saturate at 2,000 µmol photons m^{-2} s^{-1} (approximate maximum noontime irradiation) and subsequently compared gross primary production at 1,000 µmol photons m^{-2} s^{-1}. To determine whether the RLC of each clam varied as a function of clam size, we regressed the parameter α, and rETR values at 1,293 µmol photons m^{-2} s^{-1} (hereafter $rETR_{1293}$), against log-transformed tissue wet weight, added second- and third-order terms for wet weight to each regression, and used AICc to choose the most parsimonious model (Burnham and Anderson 2002) using R version 2.12.1 (R Development Core Team).

Chamber incubations

In a separate experiment, we measured photosynthetic performance using the Diving-PAM simultaneously with rates of net primary production using chamber incubations to test the relationship between photosynthesis measured from two different methods. Two cylindrical acrylic incubation chambers of approximately 330 mL in volume were constructed for the smallest clams (<5 g, $n = 4$). Chambers were equipped with pH/Oxi340i probes that automatically recorded temperature, pH, and dissolved oxygen concentrations every 5 s (WTW, Germany). Incubation chambers were kept in flow-through outdoor tanks similar to clam holding tanks, in which the entire volume was replaced every 7 min, maintaining the temperature of the incubation chambers at 29.5 ± 0.3°C (±SE), as monitored by HOBO pendant loggers (Onset, USA). Tanks were kept under clear plastic roofing exactly like the system used for fluorescence measurements, minimizing water temperature fluctuations by limiting PAR to a maximum of 654 ± 148 µmol photons m^{-2} s^{-1} (±SE) at noontime.

Prior to being placed in a chamber, clams were brushed to remove epibionts that accumulated since the original cleaning and rinsed with seawater filtered to 0.45 µm. Within the chamber, clams were placed on a small platform with a magnetic stir bar underneath and the entire chamber was placed on top of a waterproof magnetic stirrer to ensure the water in the chamber was well mixed. Cleaned

clams were placed in chambers 5 min prior to each trial to allow clams time to expand their mantle tissues and were taken out of the chambers immediately after each trial. Each clam was placed in a trial between 1 and 3 times within a 24-h period. Each trial ran for 40 min, and fresh seawater filtered to 0.45 µm was used to rinse and then fill the chambers for each trial.

Net primary production (NPP) was measured as increases in dissolved oxygen during daytime incubations, with trials taking place throughout the day each paired with 3–4 fluorescence measurements of $\Delta F/F_m'$, rETR, and PAR recorded immediately before each trial using a Diving-PAM and its calibrated light sensor. Respiration rates (R) were measured as decreases in dissolved oxygen starting at various times at least 1 h after sunset. Daytime and nighttime respiration have been found to be similar for giant clams (see Klumpp et al. 1992), so gross primary production (GPP) for each daytime trial can then be calculated as GPP = NPP + R, where R is the average of all respiration rates measured for a given clam. Each clam was placed in each incubation chamber for measurements of both NPP (2 trials clam^{-1}) and R (2 to 3 trials clam^{-1}). Clam-free controls were run at night and during the day for each chamber, and photosynthesis and respiration rates from each trial were corrected with the oxygen consumption of control trials for the corresponding chamber. Temperature and pH did not vary substantially for any given trial (temperature: 30.5 ± 0.1°C; pH: 8.22 ± 0.01 (±SE)). Oxygen levels did not fall below 80% for respiration trials and did not exceed 135% for photosynthesis trials.

We regressed GPP, NPP, and R against log-transformed tissue wet weight to illustrate the allometry of primary production and respiration. To test the relationship between photosynthesis measured by fluorescence and via chamber incubations, we used correlation followed by Model II regression on rETR against GPP, and also on NPP and $\Delta F/F_m'$ against PAR. These statistical analyses were performed using MATLAB 7.6.0.324 with Statistics Toolbox 6.2 (MathWorks, USA).

Results

Quantum yield

The small giant clam *Tridacna maxima* exhibited diel variation in photosynthetic efficiency: $\Delta F/F_m'$ values were generally high during the early morning, decreased to a low at noontime, and recovered slowly throughout the afternoon. The largest clams >50 g tissue wet weight were an exception and did not exhibit a decrease in noontime photosynthetic efficiency (Fig. 1). For visual simplicity, clams were binned into five size classes and mean ± SE $\Delta F/F_m'$
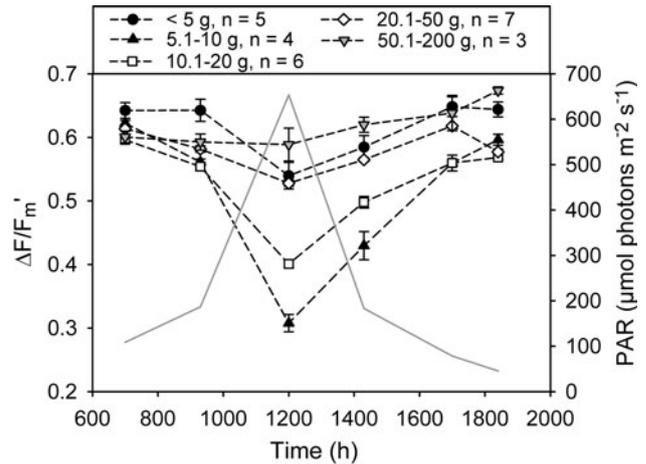

Fig. 1 Mean (±SE) effective PSII quantum yield ($\Delta F/F_m'$) for giant clams (*Tridacna maxima*) of various sizes over a 1-day period (1 Sep 2009). *Solid line* indicates mean photosynthetically active radiation (PAR, µmol photons m^{-2} s^{-1}) for each sampling time. For visual simplicity, clams are binned into five size classes based on tissue wet weight, with mean $\Delta F/F_m'$ determined by averaging measurements from 3 to 7 clams size class^{-1}, $n = 25$ clams total

values at each sampling time were plotted for each size class. Multiple regression of PAR and log-transformed tissue wet weight (as a continuous variable) as predictors of $\Delta F/F_m'$ revealed that both PAR and tissue wet weight (but not their interaction) significantly influenced $\Delta F/F_m'$ over a diel period (Multiple regression, $\Delta F/F_m' = 0.653 - 0.000159*PAR - 0.152*\log(size) + 0.0720*\log(size)^2$, $r^2 = 0.56$, ANOVA, $F_{3,146} = 61.89$, $P < 0.0001$). Thus, changes in $\Delta F/F_m'$ throughout the day are influenced by both PAR and host clam size, and high noontime PAR levels generally result in lower $\Delta F/F_m'$ values, indicating reduced photosynthetic efficiency.

Noontime decreases in $\Delta F/F_m'$, calculated as the maximum excitation pressure over PSII at noon (Q_m), varied as a quadratic function of tissue wet weight (Fig. 2). The model with an additional third-order term for wet weight resulted in an AICc score that differed from the lowest AICc score by ≤2 ($\Delta_i = -1.87$), so we chose the second-order model as the most parsimonious. Q_m increased as clam wet weight increased up to ∼10 g then decreased as wet weight increased up to 200 g. The lowest calculated Q_m value of 0.022 was recorded from a 49.7 g clam. Clams ranging from 5 to 10 g exhibited the highest values of Q_m (0.57 for a 6.54 g clam) and thus the largest decreases in noontime photosynthetic efficiency, suggesting that clams of these sizes are the most sensitive to high irradiance levels.

Rapid light curves

To illustrate the general shape of the RLCs, we binned clams into five size classes and calculated the mean ± SE
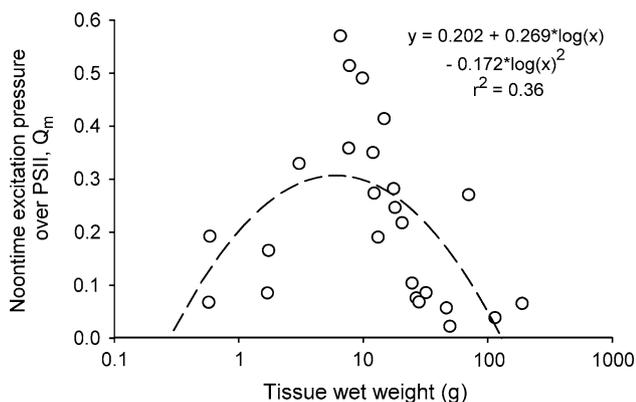
Fig. 2 PSII excitation pressure, Q_m, in giant clams, *Tridacna maxima*, calculated as $1-$(noontime $\Delta F/F_m')/(F_v/F_m$ at dusk). Q_m increased as wet weight increased up to ~ 10 g, was highest for clams ~ 5–10 g, and then decreased as wet weight increased up to 200 g (quadratic regression, $r^2 = 0.36$, $F_{2,22} = 6.159$, $P < 0.01$)
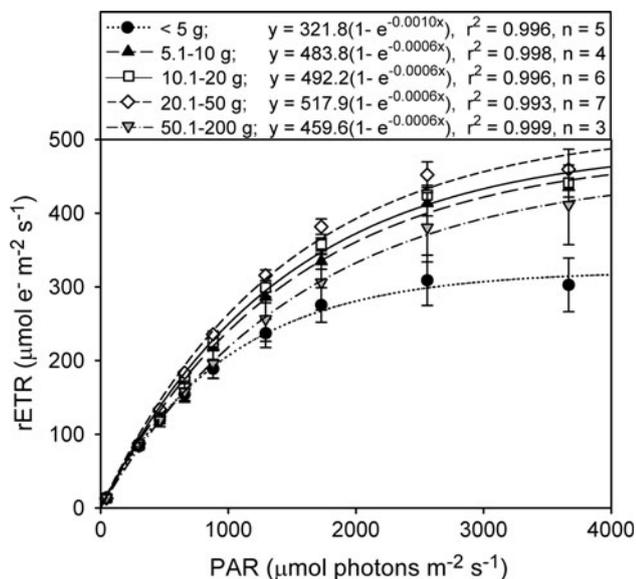
Fig. 3 Rapid light curves (RLC), rETR versus PAR, for giant clams (*Tridacna maxima*) dark adapted for at least 30 min. Mean ($\pm$SE) rETR is average of 3 to 7 clams size class^{-1}, binned by wet tissue weight for visual simplicity, $n = 25$ clams total. Standard rectangular hyperbola curves were fitted for each size class. Only 8 out of 25 RLCs reached saturation; 4 of these clams were in the smallest size class

rETR values for each actinic light intensity in each size class (Fig. 3). We also fit standard rectangular hyperbola curves for the RLCs of each of these five size classes, and for the RLC of each individual clam ($n = 25$, not shown). In all cases, rapid light curves were accurately described by standard rectangular hyperbola curves (all curves: $r^2 > 0.99$, $P < 0.0001$). For the RLCs fit for each individual clam, the maximum photochemical conversion efficiency, α, did not vary as a function of clam wet weight

($P = 0.24$). Across all clams, values for α ranged from 0.260 to 0.408 and averaged 0.341 ± 0.006 ($\pm$SE, $n = 25$) changes in rETR for a given change in PAR (μmol e^- m^{-2} s^{-1}/μmol photons m^{-2} s^{-1}).

The RLCs of only 8 out of 25 clams reached saturation and exhibited a decrease in rETR during the last actinic pulse. Of these 8 clams whose RLCs reached saturation, 4 were the smallest clams <5 g wet weight, so this is the only size class that exhibited saturation when data for each size class were averaged (Fig. 3). Instead of extrapolating to and comparing rETR$_{max}$ for RLCs that did not reach saturation, we compared rETR$_{1293}$, the rETR values at the maximum irradiance level experienced by giant clams in their natural habitat (1,293 μmol photons m^{-2} s^{-1}) (Buck et al. 2002; Jantzen et al. 2008). Values of rETR$_{1293}$ vary as a quadratic function of clam wet weight and increased as clam size increased to a maximum for clams ranging from 10–50 g wet tissue weight, before decreasing again as clam size increased up to 200 g (Fig. 4a). The AICc score of the model including a third-order term for wet weight differed by a $\Delta_i = 1.93$, so we chose the second-order quadratic model as the most parsimonious one. We measured a maximum rETR$_{1293}$ of 342.7 μmol e^- m^{-2} s^{-1} for a 20.5 g clam and a minimum rETR$_{1293}$ of 168.5 μmol e^- m^{-2} s^{-1} for the smallest clam, 0.574 g.

Maximum photosynthetic efficiency (F_v/F_m) measured immediately prior to each RLC also varied as a quadratic function of clam tissue weight, decreased as clam size increased to the lowest F_v/F_m values for clams ~ 5–50 g tissue wet weight, and then increased as clam size increased up to 200 g (Fig. 4b). Because the AICc score for the model that included a third-order term for wet weight differed by a $\Delta_i = 1.60$, we again chose the second-order quadratic model as the most parsimonious one. The maximum recorded F_v/F_m value was 0.68 for a 0.586 g clam, and the minimum recorded value was 0.55 for a 26.6 g clam. The size range of clams with the lowest maximum photosynthetic efficiencies (5–50 g) coincides with the size range of clams with the highest rETR$_{1293}$ values (10–50 g) and partly coincides with the size range of clams with the highest noontime decreases in photosynthetic efficiency (5–10 g).

Chamber incubations

Respiration and gross primary production decreased allometrically as clam size increased (Fig. 5), similarly documented by Fisher et al. (1985). Positive net primary production (NPP, in μmol O$_2$ g^{-1} min^{-1}) occurred for all daytime trials and also decreased allometrically as a function of tissue wet weight (in g): NPP $= 0.362x^{0.926}$ ($r^2 = 0.92$, $F_{1,6} = 68.90$, $P < 0.001$) (not shown). Both net primary production and photosynthetic efficiency ($\Delta F/F_m'$)
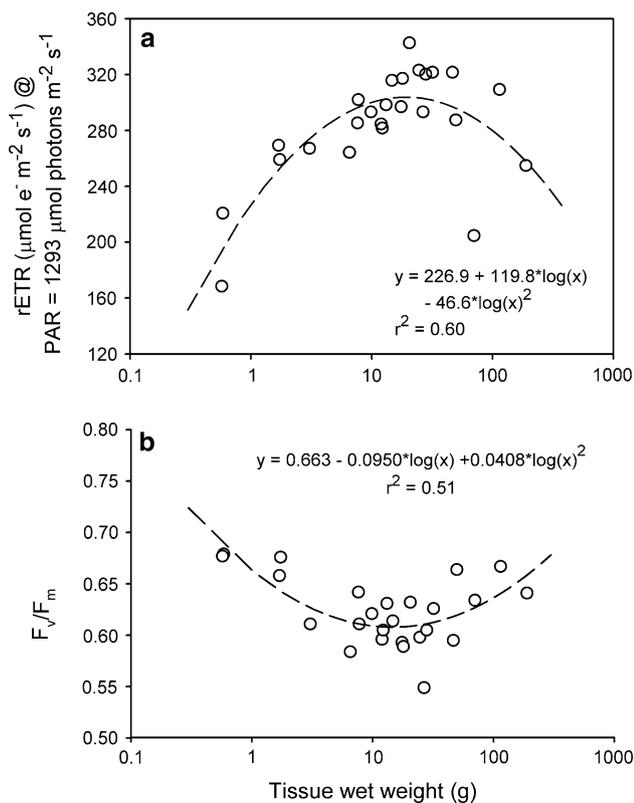
Fig. 4 **a** Relative electron transport rates (rETR, μmol e^- m^{-2} s^{-1}) at a PAR level of 1,293 μmol photons m^{-2} s^{-1} measured from RLCs. rETR$_{1293}$ increased as wet weight increased up to ~ 10 g, reached a maximum for clams ~ 10–50 g, and decreased as wet weight increased up to 200 g (quadratic regression, $r^2 = 0.60$, $F_{2,22} = 16.52$, $P < 0.0001$). **b** Dark-adapted maximum quantum yield, F_v/F_m, for *Tridacna maxima*. F_v/F_m decreased as wet weight increased up to ~ 5 g, reached a minimum for clams ~ 5–50 g, and increased slightly as wet weight increased from 50 to 200 g (quadratic regression, $r^2 = 0.51$, $F_{2,22} = 11.21$, $P < 0.001$)
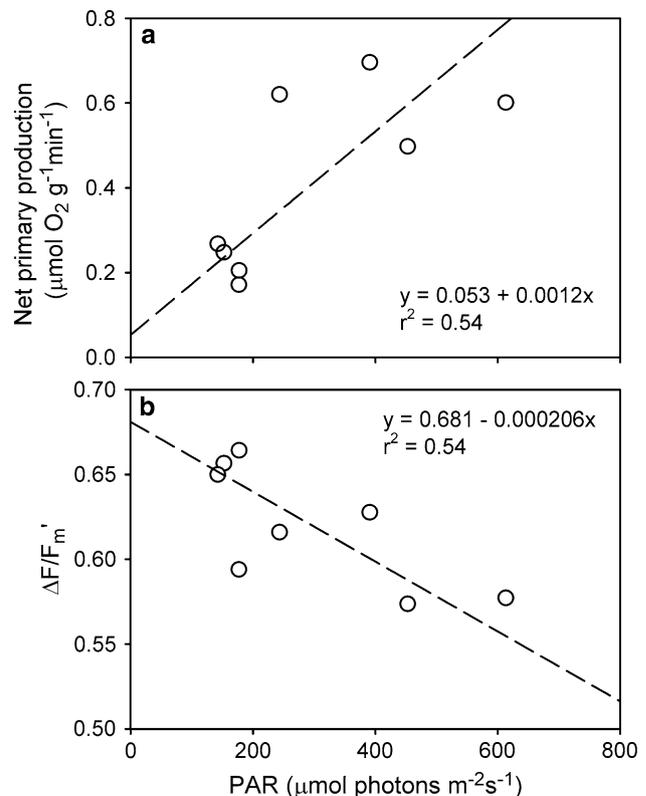
were correlated with PAR, with net primary production correlated positively (Fig. 6a) and photosynthetic efficiency correlated negatively (Fig. 6b). Fluorescence measurements of photosynthesis in the form of relative electron transport rates measured at the start of each chamber incubation were positively correlated with measurements of gross primary production from those chamber incubations (Fig. 7).

Discussion

We found size-dependent photosynthetic performance for symbionts of the giant clam, *Tridacna maxima*. Light-dependent noontime decreases in effective quantum yield, maximum quantum yield, and relative electron transport rates of giant clam symbionts varied as a quadratic function of giant clam size. Symbionts in mid-sized clams ranging from ~ 5–50 g exhibited the lowest maximum quantum
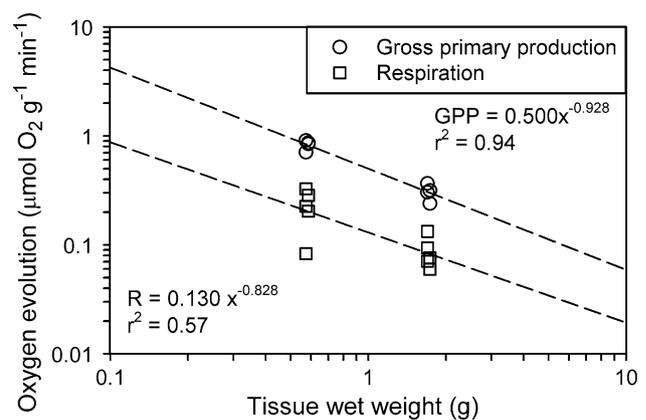
Fig. 5 Rates of gross primary production (oxygen production, *circles*, 8 trials) and respiration (oxygen consumption, *squares*, 10 trials) in units of μmol O$_2$ g^{-1} min^{-1}, obtained from chamber incubations of four juvenile giant clams, *Tridacna maxima*. Gross primary production (GPP) decreased as a function of clam size (linear regression, $r^2 = 0.94$, $F_{1,6} = 97.97$, $P < 0.0001$). Respiration (R) decreased as a function of clam size (linear regression, $r^2 = 0.57$, $F_{1,8} = 10.54$, $P = 0.012$)

Fig. 6 **a** Measurements of net primary production (oxygen evolution, μmol O$_2$ g^{-1} min^{-1}) from incubation chamber trials of juvenile giant clams, *Tridacna maxima*, were positively correlated with PAR (Model II regression, $r^2 = 0.54$, $P = 0.039$). **b** Effective PSII quantum yield ($\Delta F/F_m'$) measurements taken with a Diving-PAM at the start of each daytime chamber incubation were negatively correlated with PAR (Model II regression, $r^2 = 0.54$, $P = 0.037$)
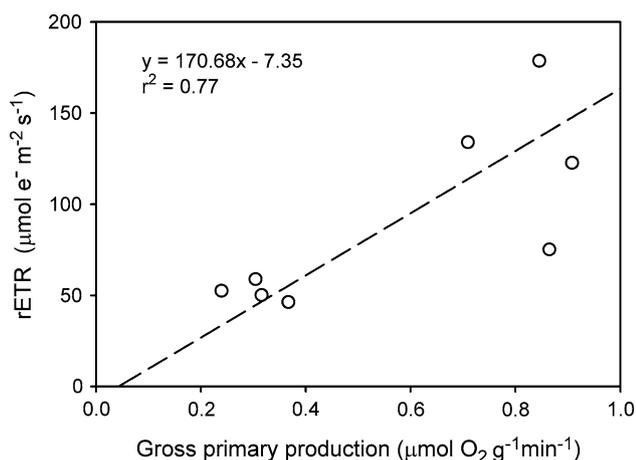
Fig. 7 Measurements of relative electron transport rates (rETR, $\mu\text{mol e}^- \text{ m}^{-2} \text{ s}^{-1}$) taken with a Diving-PAM at the start of each daytime chamber incubation were positively correlated with measurements of gross primary production ($\mu\text{mol O}_2 \text{ g}^{-1} \text{ min}^{-1}$) from those chamber incubations (Model II regression, $r^2 = 0.77$, $P = 0.02$)

yields, the highest noontime decreases in yield, and the highest relative electron transport rates at the maximum irradiance level experienced by giant clams in their natural habitat. In contrast, symbionts in the largest clams >50 g and smallest clams <5 g exhibited higher maximum quantum yields, smaller noontime decreases in yield, and lower relative electron transport rates.

Light-dependent noontime decreases in photosynthetic efficiency calculated as Q_m varied as a quadratic function of clam size, and Q_m was highest for clams ~ 10 g tissue wet weight, with a maximum value of 0.57 (values close to 1.0 suggest photoinhibition). Photoinhibition is the light-dependent reversible reduction of photosynthetic efficiency that entails either reversible damage and repair of PSII or the induction of mechanisms protective of PSII via decreased absorption of light energy or increased thermal dissipation (Critchley 2000). An alternative, more likely explanation for the light-dependent reduction of photosynthetic efficiency, is down-regulation of PSII by light-induced acidification (ΔpH) of the lumen in chloroplast thylakoids (Öquist et al. 1992; van Wijk and van Hasselt 1993). The energetic cost of reduced electron transport rates in corals, organisms that also host *Symbiodinium*, was found to be negligible (Hoogenboom et al. 2006), so it is unlikely that changes in Q_m are responsible for the allometric increase in symbiont contribution to giant clam respiratory requirements as clam size increases. Jantzen et al. (2008) documented a higher Q_m value for *T. maxima* clams ~ 200 g compared to our findings ($Q_m \sim 0.33$, compared to $Q_m < 0.10$ measured here), and this discrepancy is likely caused by the higher noontime irradiance in Jantzen et al.'s study ($\sim 1,000 \mu\text{mol photons m}^{-2} \text{ s}^{-1}$

compared to 654 $\mu\text{mol photons m}^{-2} \text{ s}^{-1}$ measured here) (see Iglesias-Prieto et al. 2004).

While our results reveal size-dependent variation in symbiont photosynthetic performance in giant clams, the quadratic patterns we found do not readily explain the allometric relationship between symbiont contribution to clam respiratory requirements and host clam size. Based on a positive correlation between relative electron transport rates and gross primary production, and the allometric decrease in gross primary production as clam size increased, we would expect that relative electron transport rates decreased allometrically as clam size increased, rather than varying as a quadratic function of clam size. The pattern of decreasing electron transport rates as clam size increased holds for symbionts in clams >50 g but does not hold for symbionts in smaller clams. We would also expect symbionts with the highest electron transport rates in mid-sized clams ~ 5–50 g to also exhibit high maximum photosynthetic efficiencies, when they actually exhibited some of the lowest maximum photosynthetic efficiencies. We posit three mechanisms (or a combination thereof) to explain the size-dependent variation in symbiont photosynthetic performance: (a) size-dependent changes in the physiology of symbiosis, (b) size-dependent changes in in situ light regimes, and (c) symbiont sub-clade genetic variation.

The physiology of symbiosis between symbionts and their clam hosts may change and develop as a function of clam size. Evidence for this can be found in the dynamics of the uptake of ammonium, an essential limiting nutrient for photosynthetic symbionts, as a function of clam size. Ammonium uptake per symbiont and symbiont density were found to vary with clam size and were low for the smallest *T. gigas* clams, increased as clam size increased to maximum values for juvenile clams and then decreased gradually as clam size increased (Fitt et al. 1993). Thus, small clams with the highest symbiont densities also exhibited the highest ammonium uptake rates per symbiont and vice versa, indicating that the degree of nutrient uptake is size-dependent. Even though the smallest clams contained symbionts that took up ammonium, these clams exhibited a net emission of ammonium compared to the increasing net uptake of ammonium as clam size increased in larger clams (Fitt et al. 1993; Hawkins and Klumpp 1995), suggesting that the tight coupling of nutrient recycling between symbionts and their clam hosts was not achieved yet in juvenile clams, or that there were insufficient numbers of symbionts in juvenile clams to take up all the ammonium released by their host clam. Thus, the physiology of the symbiont-clam symbiosis may change as a function of clam size and could serve as a mechanism for the quadratic patterns of photosynthetic performance measured here.

Size-dependent variation in photosynthetic performance could also be caused by size-dependent differences in in situ light regimes: increased internal shading of symbionts can occur via a thickening of clam mantle tissue or change in tissue opacity, reducing actual light levels reaching symbionts. Fisher et al. (1985) found evidence of increased shading of symbionts as clam size increased over part of the size range of *T. gigas*, by showing gross primary production per zooxanthellae was negatively correlated with clam size, and by comparing P–I curves of isolated symbionts to P–I curves of symbionts in situ. In addition, symbionts themselves may exist in multiple layers (Trench et al. 1981), so shading by other symbionts may also occur. We found a negative correlation between effective quantum yield and light levels, supporting the idea that reduced light levels from increased internal shading as clam size increased would result in higher measurements of photosynthetic efficiency, and thus, smaller noontime decreases in photosynthetic efficiency, as clam size increased. Size-dependent differences in in situ light regimes could also explain size-dependent changes in rETR. To calculate rETR, we assumed the fraction of light absorbed by clam tissue was constant with size ($A = 1$), but this light absorptance may change depending on the thickness and opacity of mantle tissue. If shading increases as clam size increases, we overestimated the light absorptance for larger clams and may have overestimated rETR. Factoring in the exact absorptance may reduce observed differences in rETR (Cayabyab and Enríquez 2007). In situ light levels would have to vary as a quadratic function of clam size to explain our results, so while size-dependent changes in in situ light regimes likely occur, they are not the only mechanism responsible for the observed patterns.

Another potential cause of the observed size-dependent differences in photosynthetic performance is symbiont sub-clade genetic variation. Giant clam symbionts can be divided into several distinct groups, or clades (Pochon and Gates 2010). Our study species *T. maxima* has only been found to harbor clade A symbionts (Carlos et al. 1999; Baillie et al. 2000), while other species of giant clam harbor either clade A or C symbionts with the exception of *T. crocea* that associates with both clade A and C (although not both in the same individual) (Rowan 1998; Carlos et al. 1999; Baillie et al. 2000). While photosynthetic efficiency measured via chlorophyll fluorescence has recently been found to differ *between* clades (Abrego et al. 2008; Cantin et al. 2009), determining differences in photosynthetic efficiency *within* a clade, and whether symbiont sub-clade differs as a function of clam size, is precluded by the lack of a standardized classification of *Symbiodinium* at the sub-clade level.

We found a significant correlation between chlorophyll fluorescence measurements of relative electron transport rates and chamber incubation measurements of gross primary production. Similar relationships between rETR and gross primary production were found in other studies of giant clams (Jantzen et al. 2008), and also for other photosynthetic organisms (see introduction). The variability around the rETR-GPP relationship indicates a degree of error in inferring rates of gross primary production strictly from fluorescence measurements. Variation around measurements of GPP can be confounded by alternative electron transport pathways, such as the Mehler reaction of PSI that reduces O_2 to H_2O using electrons from PSII, dissipates excess excitation energy in the process, and can result in net oxygen uptake when the enzymes necessary to break down intermediate products are inhibited (Asada 1999; Raghavendra 2000). Another alternative electron transport pathway that could confound measurements of GPP is the cyclic electron transport pathway of PSI that results in a decrease in oxygen evolution as electrons are cycled through PSI to create ATP (Raghavendra 2000). We also found variability around the NPP-PAR and $\Delta F/F_m'$-PAR correlations, suggesting other factors besides PAR influence NPP and $\Delta F/F_m'$ in hospite.

Overall, our results indicate that chlorophyll fluorescence measurements of Q_m, F_v/F_m, and rETR from symbionts vary with giant clam size, and size must be controlled for when these measurements are compared among conspecific individuals. Our paper provides background for further studies of three mechanisms causing the quadratic patterns of photosynthetic performance as a function of clam size. We hypothesize that size-dependent changes in the physiology of symbiosis, in situ light regimes, or symbiont sub-clade genetic variation, or a combination thereof, are responsible for the observed patterns in photosynthetic performance. Studies of giant clam photophysiology are important to understanding their growth and survival and are vital to worldwide aquaculture efforts of these bivalves that are disappearing due to human harvest for consumption and the aquarium trade (Johannes 1978; Lucas 1994). Our study sheds new light on size-dependent changes in *Symbiodinium* photosynthetic performance within giant clams and contributes to our general knowledge of algal-invertebrate symbioses.

anonymous reviewers for helpful comments that improved earlier versions of this manuscript. These studies complied with current laws of Taiwan, ROC, and the authors declare no conflict of interest.

References

Abrego D, Ulstrup KE, Willis BL, Van Oppen MJH (2008) Species–specific interactions between algal endosymbionts and coral hosts define their bleaching response to heat and light stress. Proc R Soc Biol Sci Ser B 275:2273

Andrefouet S, Gilbert A, Yan L, Remoissenet G, Payri C, Chancerelle Y (2005) The remarkable population size of the endangered clam *Tridacna maxima* assessed in Fangatau Atoll (Eastern Tuamotu, French Polynesia) using in situ and remote sensing data. ICES J Mar Sci 62:1037–1048

Anthony K, Hoegh-Guldberg O (2003) Kinetics of photoacclimation in corals. Oecologia 134:23–31

Asada K (1999) The water–water cycle in chloroplasts: scavenging of active oxygens and dissipation of excess photons. Annu Rev Plant Physiol Plant Mol Biol 50:601–639

Baillie BK, Belda-Baillie CA, Maruyama T (2000) Conspecificity and Indo-Pacific distribution of *Symbiodinium* genotypes (Dinophyceae) from giant clams. J Phycol 36:1153–1161

Beer S, Larsson C, Poryan O, Axelsson L (2000) Photosynthetic rates of *Ulva* (Chlorophyta) measured by pulse amplitude modulated (PAM) fluorometry. Eur J Phycol 35:69–74

Buck BH, Rosenthal H, Saint-Paul U (2002) Effect of increased irradiance and thermal stress on the symbiosis of *Symbiodinium microadriaticum* and *Tridacna gigas*. Aquat Living Resour 15:107–117

Burnham KP, Anderson DR (2002) Model selection and multimodel inference: a practical information—theoretic approach. Springer, New York

Cantin N, van Oppen M, Willis B, Mieog J, Negri A (2009) Juvenile corals can acquire more carbon from high-performance algal symbionts. Coral Reefs 28:405–414

Carlos AA, Baillie BK, Kawachi M, Maruyama T (1999) Phylogenetic position of *Symbiodinium* (Dinophyceae) isolates from Tridacnids (Bivalvia), Cardiids (Bivalvia), a sponge (Porifera), a soft coral (Anthozoa), and a free-living strain. J Phycol 35:1054–1062

Cayabyab NM, Enríquez S (2007) Leaf photoacclimatory responses of the tropical seagrass *Thalassia testudinum* under mesocosm conditions: a mechanistic scaling-up study. New Phytol 176:108–123

Critchley C (2000) Photoinhibition. In: Raghavendra AS (ed) Photosynthesis. A comprehensive treatise. Cambridge University Press, Cambridge, pp 264–272

Elfwing T, Blidberg E, Tedengren M (2002) Physiological responses to copper in giant clams: a comparison of two methods in revealing effects on photosynthesis in zooxanthellae. Mar Environ Res 54:147–155

Elfwing T, Blidberg E, Sison M, Tedengren M (2003) A comparison between sites of growth, physiological performance and stress responses in transplanted *Tridacna gigas*. Aquaculture 219:815–828

Enríquez S, Borowitzka MA (2010) The use of the fluorescence signal in studies of seagrasses and macroalgae. In: Suggett DJ, Prášil O, Borowitzka MA (eds) Chlorophyll *a* fluorescence in aquatic sciences: methods and applications. Springer, Netherlands, pp 187–208

Fisher CR, Fitt WK, Trench RK (1985) Photosynthesis and respiration in *Tridacna gigas* as a function of irradiance and size. Biol Bull 169:230–245

Fitt WK, Trench RK (1981) Spawning, development, and acquisition of zooxanthellae by *Tridacna squamosa* (Mollusca, Bivalvia). Biol Bull 161:213–235

Fitt WK, Rees TAV, Braley RD, Lucas JS, Yellowlees D (1993) Nitrogen flux in giant clams: Size-dependency and relationship to zooxanthellae density and clam biomass in the uptake of dissolved inorganic nitrogen. Mar Biol 117:381–386

Genty B, Briantais J-M, Baker NR (1989) The relationship between the quantum yield of photosynthetic electron transport and quenching of chlorophyll fluorescence. Biochim Biophys Acta 990:87–92

Griffiths CL, Klumpp DW (1996) Relationships between size, mantle area and zooxanthellae numbers in five species of giant clam (Tridacnidae). Mar Ecol Prog Ser 137:139–147

Hawkins AJS, Klumpp DW (1995) Nutrition of the giant clam *Tridacna gigas* (L.). II. Relative contributions of filter-feeding and the ammonium-nitrogen acquired and recycled by symbiotic alga towards total nitrogen requirements for tissue growth and metabolism. J Exp Mar Biol Ecol 190:263–290

Hoogenboom MO, Anthony KRN, Connolly SR (2006) Energetic cost of photoinhibition in corals. Mar Ecol Prog Ser 313:1–12

Iglesias-Prieto R, Beltran VH, LaJeunesse TC, Reyes-Bonilla H, Thome PE (2004) Different algal symbionts explain the vertical distribution of dominant reef corals in the Eastern Pacific. Proc R Soc Biol Sci Ser B 271:1757–1763

Ishikura M, Adachi K, Maruyama T (1999) Zooxanthellae release glucose in the tissue of a giant clam, *Tridacna crocea*. Mar Biol 133:665–673

Jantzen C, Wild C, El-Zibdah M, Roa-Quiaoit H, Haacke C, Richter C (2008) Photosynthetic performance of giant clams, *Tridacna maxima* and *T. squamosa*, Red Sea. Mar Biol 155:211–221

Jeffrey SW, Haxo FT (1968) Photosynthetic pigments of symbiotic dinoflagellates (zooxanthellae) from corals and clams. Biol Bull 135:149–165

Johannes RE (1978) Traditional marine conservation methods in Oceania and their demise. Annu Rev Ecol Syst 9:349–364

Klumpp DW, Griffiths CL (1994) Contributions of phototrophic and heterotrophic nutrition to the metabolic and growth requirements of four species of giant clam (Tridacnidae). Mar Ecol Prog Ser 115:103–115

Klumpp DW, Lucas JS (1994) Nutritional ecology of the giant clams *Tridacna tevoroa* and *T. derasa* from Tonga—influence of light on filter-feeding and photosynthesis. Mar Ecol Prog Ser 107:147–156

Klumpp DW, Bayne BL, Hawkins AJS (1992) Nutrition of the giant clam *Tridacna gigas* (L.). I. Contribution of filter feeding and photosynthates to respiration and growth. J Exp Mar Biol Ecol 155:105–122

Lucas JS (1994) The biology, exploitation, and mariculture of giant clams (Tridacnidae). Rev Fish Sci 2:181–223

Maxwell K, Johnson GN (2000) Chlorophyll fluorescence-a practical guide. J Exp Bot 51:659–668

Morton B (1978) The diurnal rhythm and the processes of feeding and digestion in *Tridacna crocea* (Bivalvia: Tridacnidae). J Zool 185:371–387

Norton JH, Shepherd MA, Long HM, Fitt WK (1992) The zooxanthellal tubular system in the giant clam. Biol Bull 183:503–506

Öquist G, Chow WS, Anderson JM (1992) Photoinhibition of photosynthesis represents a mechanism for the long-term regulation of photosystem II. Planta 186:450–460

Pochon X, Gates RD (2010) A new *Symbiodinium* clade (Dinophyceae) from soritid foraminifera in Hawai'i. Mol Phylogenet Evol 56:492–497

Raghavendra AS (ed) (2000) Photosynthesis: a comprehensive treatise. Cambridge University Press, Cambridge

Ralph PJ, Gademann R (2005) Rapid light curves: a powerful tool to assess photosynthetic activity. Aquat Bot 82:222–237

Reid RGB, Fankboner PV, Brand DG (1984) Studies on the physiology of the giant clam *Tridacna gigas* Linne—I. Feeding and digestion. Comp Biochem Physiol 78A:95–101

Richter C, Roa-Quiaoit H, Jantzen C, Al-Zibdah M, Kochzius M (2008) Collapse of a new living species of giant clam in the Red Sea. Curr Biol 18:1349–1354

Rosewater J (1965) The family Tridacnidae in the Indo-Pacific. Indo-Pacific, Mollusca, pp 347–394

Rowan R (1998) Review: diversity and ecology of zooxanthellae on coral reefs. J Phycol 34:407–417

Schreiber U (2004) Pulse-amplitude-modulation (PAM) fluorometry and saturation pulse method: an overview. In: Papageorgiou G, Govindjee (eds) Chlorophyll *a* fluorescence: a signature of photosynthesis. Springer, Dordrecht, pp 279–319

Trench RK (1993) Microalgal-invertebrate symbioses: a review. Endocytobio Cell Res 9:135–175

Trench RK, Wethey DS, Porter JW (1981) Observations on the symbiosis with zooxanthellae among the Tridacnidae (Mollusca, Bivalvia). Biol Bull 161:180–198

van Wijk K, van Hasselt P (1993) Photoinhibition of photosystem II in vivo is preceded by down-regulation through light-induced acidification of the lumen: consequences for the mechanism of photoinhibition in vivo. Planta 189:359–368

Venn AA, Loram JE, Douglas AE (2008) Photosynthetic symbioses in animals. J Exp Bot 59:1069–1080

White AJ, Critchley C (1999) Rapid light curves: a new fluorescence method to assess the state of the photosynthetic apparatus. Photosynth Res 59:63–72